

Supplementary Information for:

Large thermoelectric power factors and impact of texturing on the thermal conductivity in polycrystalline SnSe

S. R. Popuri¹, M. Pollet^{2,3}, R. Decourt^{2,3}, F. D. Morrison⁴, N. S. Bennett⁵, and J. W. G. Bos¹

1. Institute of Chemical Sciences and Centre for Advanced Energy Storage and Recovery, School of Engineering and Physical Sciences, Heriot-Watt University, Edinburgh, EH14 4AS, UK.

2. CNRS, ICMCB, UPR 9048, Pessac F-33600, France.

3. University of Bordeaux, UPR 9048, Pessac F-33600, France.

4. EaStCHEM School of Chemistry, University of St Andrews, St Andrews, KY16 9ST, UK.

5. Nano-Materials Lab., Institute of Mechanical, Process & Energy Engineering, School of Engineering & Physical Sciences, Heriot-Watt University, Edinburgh EH14 4AS, UK.

Table S1: Refined lattice and atomic parameters for SnSe. Data obtained from Rietveld fits against X-ray powder diffraction data.

T (K)	Lattice parameters (\AA)			Sn			Se		100* U_{iso} (\AA^2)	χ^2
	a	b	c	x	z	z	z	z		
298	11.4996(3)	4.4454(3)	4.1550(3)	0.1195(1)	0.101(1)	0.8583(2)	0.478(2)	2.8(1)	5.3	
348	11.5143(4)	4.4409(3)	4.1617(3)	0.1197(1)	0.100(1)	0.8582(2)	0.480(2)	3.1(1)	5.2	
398	11.5300(4)	4.4368(3)	4.1689(4)	0.1199(1)	0.097(1)	0.8585(2)	0.482(2)	3.6(1)	5.1	
448	11.5464(4)	4.4294(4)	4.1780(4)	0.1201(2)	0.094(1)	0.8585(2)	0.482(2)	3.6(1)	5.2	
498	11.5636(4)	4.4216(4)	4.1873(4)	0.1203(2)	0.091(2)	0.8587(2)	0.486(2)	3.9(1)	5.2	
548	11.5827(4)	4.4127(4)	4.1979(5)	0.1205(2)	0.091(2)	0.8586(2)	0.483(2)	4.1(1)	5.3	
598	11.6030(4)	4.3996(4)	4.2114(5)	0.1210(2)	0.086(1)	0.8588(2)	0.483(2)	4.5(1)	5.1	
648	11.6257(4)	4.3854(4)	4.2273(5)	0.1216(2)	0.079(1)	0.8589(3)	0.480(2)	4.8(1)	5.1	
698	11.6498(5)	4.3664(4)	4.2470(5)	0.1222(2)	0.069(2)	0.8594(3)	0.483(3)	5.4(1)	5.0	
748	11.6778(5)	4.3400(4)	4.2740(5)	0.1231(2)	0.055(2)	0.8598(3)	0.488(3)	5.7(1)	5.2	
798	11.7127(4)	4.3010(4)	4.3113(4)	0.1241(2)	0	0.8603(3)	0.5(0)	5.6(1)	5.0	
848	11.7251(4)	4.3034(3)	4.3179(4)	0.1242(2)	0	0.8605(3)	0.5(0)	5.9(1)	3.5	

Fig. S1. Photographs of the SnSe ingots studied in this manuscript (ingots #1,2 are shown in the left hand side image, ingot #3 in the right hand side image).

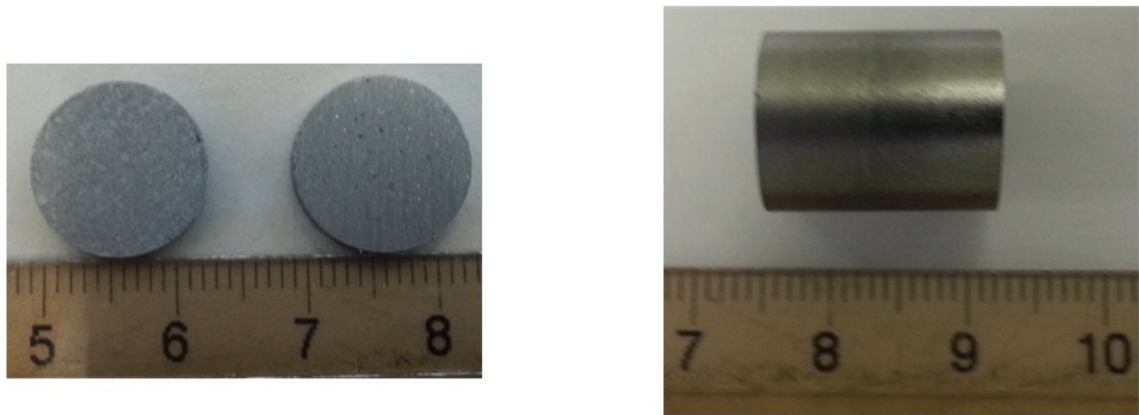


Fig. S2. Close-up of X-ray powder diffraction patterns collected on bars cut from ingots 1 and 3.

Data are shown for faces parallel and perpendicular to the hot-press direction as illustrated in Figure 1 of the manuscript.

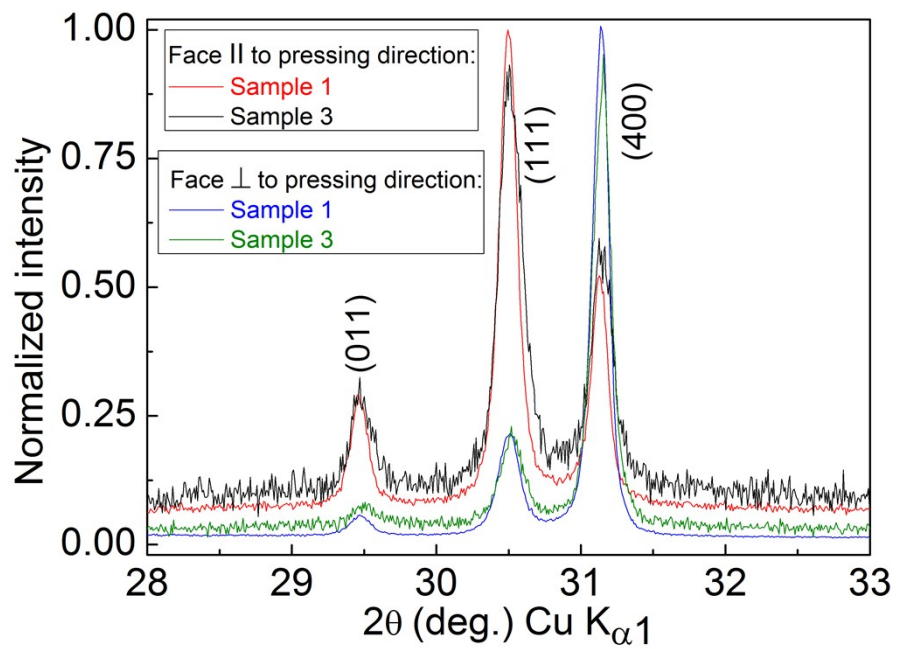


Fig. S3. SEM study of a bar cut parallel to the pressing direction from ingot 3. This illustrates the presence of coherent domains of SnSe platelets oriented at ~45 degrees with respect to the hot-press direction. This coherent stacking of platelets is lost near the bottom surface of the pellet (image 4).

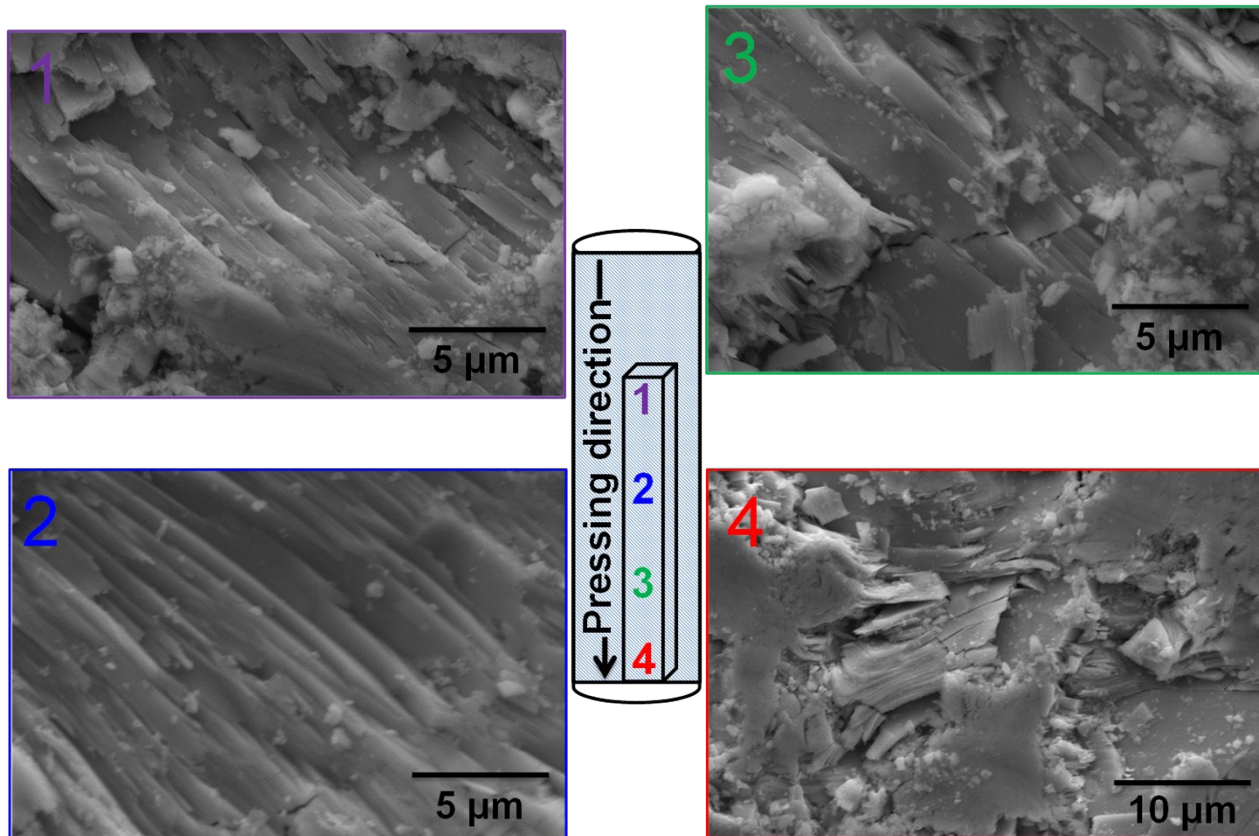


Fig. S4. Temperature dependence of the heat capacity of SnSe.

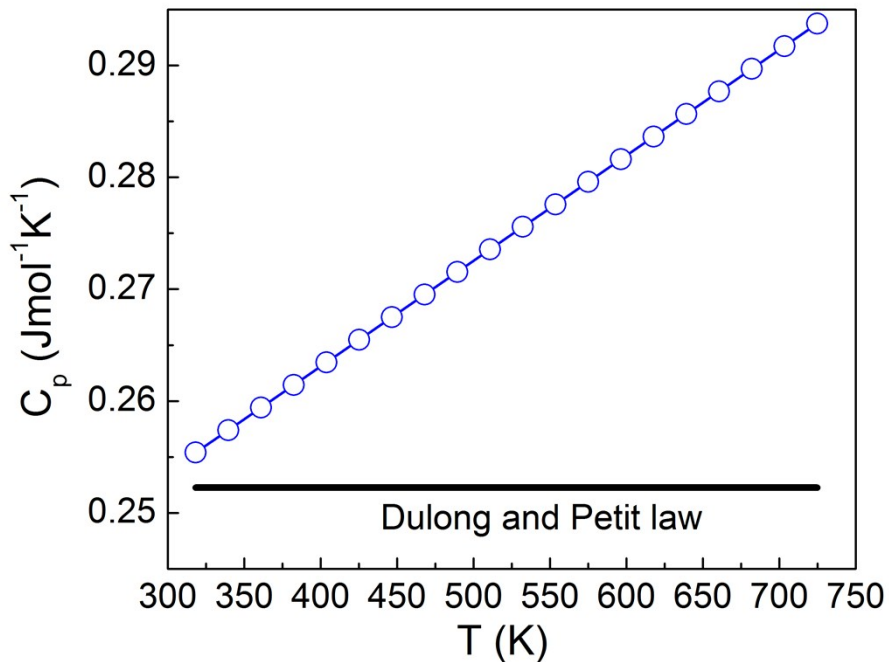


Fig. S5. Temperature dependence of the total (κ), lattice (κ_{lat}) and electronic (κ_{el}) thermal conductivity for SnSe. Data collected in the perpendicular to pressing direction, on a disc cut from ingot 3. κ_{lat} was estimated using the Wiedemann-Franz law: $\kappa_{\text{lat}} = \kappa \cdot L \sigma T$, where L is the Lorenz number, σ is the electrical conductivity, and T is the absolute temperature. ($L = 2.5 \times 10^{-8} \text{ V}^2 \text{ K}^{-2}$).

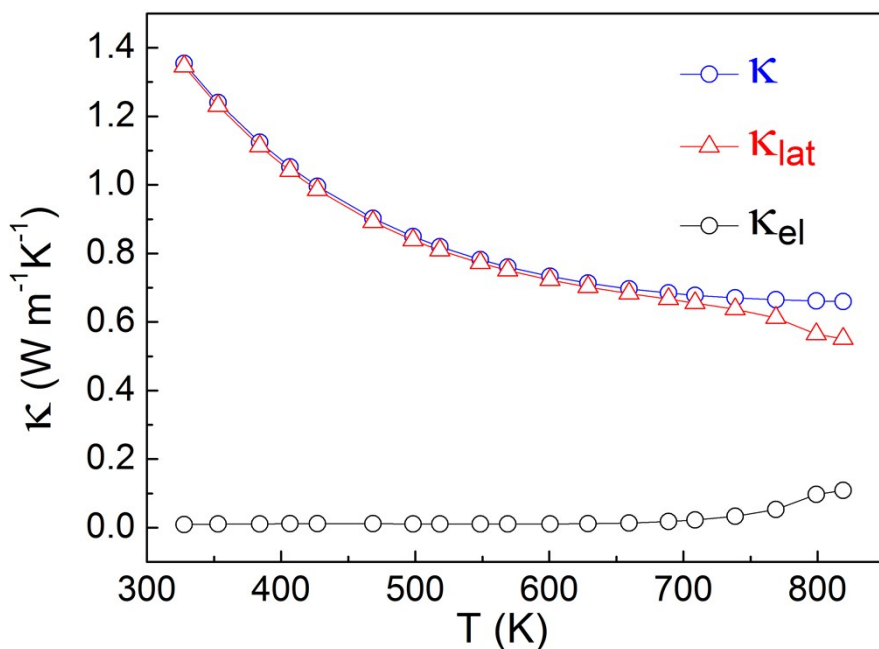


Fig. S6: Observed (open circles), calculated (red line) and difference (green line) Rietveld profiles for room temperature X-ray powder diffraction data collected on SnSe. Texturing was modelled using spherical harmonics preferential orientation coefficients. Data collected using a PANalytical Empyrean diffractometer (Mo $K_{\alpha 1,\alpha 2}$).

